OIL SPILL DETECTION IN THE CASPIAN SEA WITH A SAR IMAGE USING A DENSENET MODEL

F. Barzegar [1*], S. T. Seydi [1], S. Farzaneh [1], M. A. Sharifi [1]

[1] School of Surveying and Geospatial Engineering, College of Engineering, University of Tehran, Tehran, Iran - (fatemebarzegar, seydi.teymoor, farzaneh, Sharifi)@ut.ac.ir

Commission IV, WG IV/3

KEY WORDS: Oil Spill, Remote Sensing, Machine Learning, SAR Image, Convolutional Neural Network (CNN), DenseNet.

ABSTRACT:

Hydrocarbon spills play a vital part in contaminating water resources such as the seas and oceans. Establishing a quick and accurate approach to identifying hydrocarbons is critical to addressing these pollutants' harmful effects on the aquatic environment and local residents. The use of satellite remote sensing to detect large-scale oil spills is one of the most extensively used domains for this purpose. A machine learning method with high speed and accuracy was proposed in this study to detect occurring hydrocarbon leaks in a SAR image captured by the Sentinel-1A satellite in the Caspian Sea. The suggested method is a dense-structured network of deep learning (DenseNet) that takes the required image as input and divides it into two classes, namely, oil Spill and non-oil Spill. This dense Network outperforms the standard convolutional neural network algorithm (CNN). As a result of using the Sentinel-1A SAR image of the Caspian Sea, we achieved an overall accuracy of 99.83% and a Kappa coefficient of 0.9055.

1. INTRODUCTION

Oil leak accidents have been more frequent in recent years due to the growth of maritime transportation and extensive oil extraction. Oil spills have severely disrupted maritime economics, and monitoring and controlling oil pollution is costly and time-consuming. According to the points mentioned, having an accurate and quick method for detecting oil spills is critical to planning for the collection and removal of the polluted area. On the other hand, traditional approaches require a person's presence and direct contact with the contaminated environment. Due to necessity of continuous site observations to locate oil slicks, traditional approaches are expensive and time-consuming (Yekeen et al., 2020).

The use of remote sensing images for this purpose has grown in popularity as remote sensing technology has advanced in all areas required to identify oil slicks, such as spatial and temporal separation, large coverage, continuous data availability, and so on (Hassani et al., 2020). Furthermore, since passive microwave sensors do not perform well for detecting and displaying oil slicks due to their limited spatial resolution, active microwave sensors, including the most well-known radar sensors, are commonly employed to detect oil slicks.

Nowadays, SAR and optical images are the most often utilized methods for identifying oil slicks. SAR images, unlike optical images, are not impacted by weather conditions such as fog, clouds, and rain and may record high-resolution images at any time of day or night. As a result, in this study, SAR images were employed to identify oil slicks (Yu et al., 2017).

Oil slicks detected in SAR images are darker than the surrounding regions. This distinction between the oil slick and the environment aids in identifying and displaying the oil slick (Hassani et al., 2020).

With the growth of machine learning in recent years, various image recognition and classification algorithms have been introduced (Jordan and Mitchell, 2015). Machine learning, particularly deep learning, is a practical, rapid, and accurate method of extracting features that, compared to older and more widespread methods in artificial intelligence, performs better in separating oil spills from look-alikes. Among the typical deep learning approaches, Densenet has produced superior results in various aspects (Iandola et al., 2014), even in spotting oil spills.

There are numerous works in detecting oil spills; to name a few, we can mention that Orfanidis et al. (2018) that used a deep neural network to identify oil slicks in Sentinel-1 images. They semantically categorized the images into three classes oil spill, look-alike, and background and reached the accuracy of 0.8063 and 0.8166. Cantorna et al. (2019) compared neural network, clustering, and logistic regression techniques for oil spill categorization in ENVISAT and Sentinel-1A SAR images. In this instance, the neural network outperformed the other two methods by precision of 0.950. Yekeen et al. (2020) classified SAR images using a deep learning CNN Mask-Region-based model. They employed 2882 SAR images from Sentinel-1A and B satellites and classified them into four categories with an accuracy of 0.964. Zeng and Wang (2020) developed the Oil Spill Convolutional Network, a deep neural network approach (OSCNet) using SAR images. The suggested OSCNet approach outperformed existing machine learning methods in classification performance with an accuracy of 94.01%. Conceição et al. (2021) introduced a method based on two random forest classifiers testing with sentinel-1 SAR image with up to 90% accuracy. Wang et al. (2022) proposed an improved deep learning model named BO-DRNet using quad-polarimetric SAR images of RADARSAT-2, and they reached the mean accuracy of 74.69%.

This article is structured as follows: The proposed method's specifics and some of its details are presented in Section 2. The description of SAR image used in this study and the proportion

of it in every step is described in Section 3. The evaluation results are presented in Section 4, and a review of the study and results is presented in Section 5.

2. PROPOSED OIL SPILL DETECTION FRAMEWORK

In the following part, we will discuss the suggested model's specifics. This model is made up of three major sections (Figure 1). The input data, which is a SAR image, is pre-processed in the first stage before being fed into the algorithm. Following that, comes the model training stage, which is responsible for tuning the parameters to achieve the optimum model. The final result is created in the third stage, which consists of prediction and accuracy assessment, and the accuracy indices that are derived by comparing the result with the test dataset.

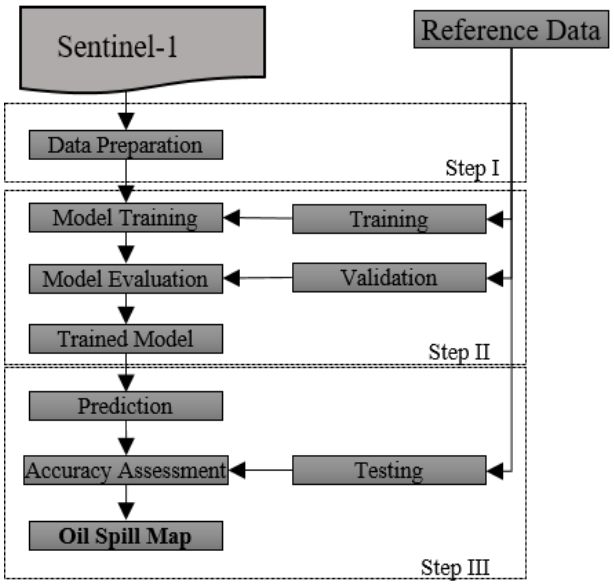

Figure 1. Flowchart of the proposed method.

2.1 Pre-processing

The Sentinel-1 Level-1 GRD SAR image must be pre-processed before it can be used in the network as an input. As a result, some of the standard pre-processing for SAR images was done to this image. This step consists of radiometric correction, de-noising, and radiometric calibration.

2.2 DenseNet

DenseNet is a network introduced by (Huang et al., 2017) that connects each layer to every other layer in a feed-forward method. In other words, DenseNet attempts to connect all layers through Dense blocks. As can be observed in Figure 2, this framework consists of three major components: (1) a dense block, (2) a transition block, and (3) a fully connected layer. The Dense block has numerous convolution layers, using the feature map of all previous layers as input and its own feature map as input to all following layers. A convolution layer and a pooling layer are included in the transition block to reduce the size of the feature map. The most recent layer is a fully connected layer whose feature map is flattened before a decision is taken by the input dataset.

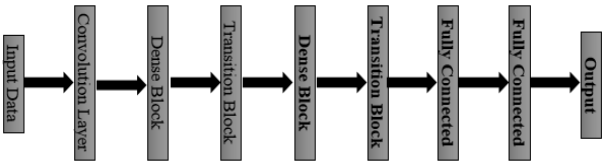

Figure 2. The architecture of DenseNet for oil spill detection.

The Dense block has a crucial role in extracting deep features, as shown in Figure 3. Based on this figure, the Dense block is included four convolution layers with beach-normalisation and rectified linear unit (ReLu) activation function.

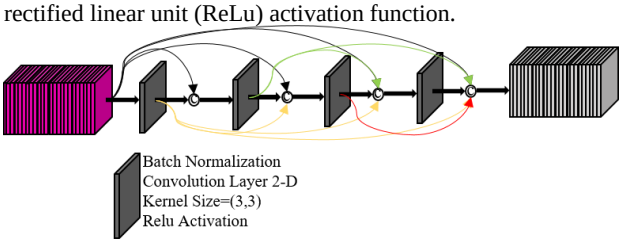

Figure 3. The structure of Dense block.

Figure 4 depicts the structure of a transition block. This block includes a convolution layer and a max-pooling layer for feature size map reduction.

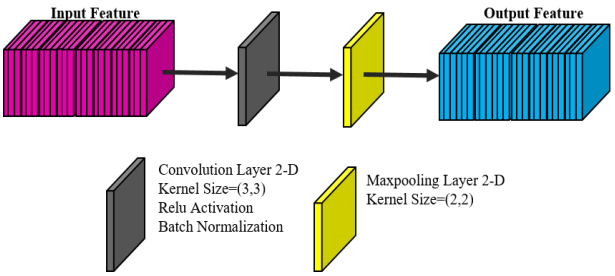

Figure 4. The structure of transition block.

2.3 Convolution layer

Extracting deep high-level features from input pictures is the primary purpose of the convolution layers. Most of the time, the convolution layers automatically analyse both spectral and spatial data (Seydi et al., 2021). The computation for a convolutional layer in the lth layer is defined by Equation 1 (Seydi et al., 2021).

$$a^l = f(w^l x^{l-1}) + b^l \quad (1)$$

where f = activation function
x = input data from layer l-1
w = weight parameter
b = bias vector

Equation 2 can be used to calculate the output of the j[th] feature map (z) in the i[th] layer at the spatial position of (x,y) in the 2D convolution layer (Ansari et al., 2021; Seydi and Hasanlou, 2021).

$$z_{i,j}^{xy} = f\left(b_{i,j} + \sum_{u} \sum_{n=0}^{N_i-1} \sum_{p=0}^{P_i-1} K_{i,j}^{n,p} v_{i-1,u}^{(x+u)(y+p)}\right) \quad (2)$$

where u = feature cube connected to the current feature cube in the $(i-1)^{th}$ layer

K = $(n, p)^{th}$ value of the kernel connected to the u^{th} feature cube in the previous layer
N = length of convolution kernel size
P = width of convolution kernel size

2.4 Accuracy Assessment

An accuracy evaluation follows the procedure of finding an oil spill. When the optimal model is found by tuning the parameters, the trained model predicts from the test data. The predicted result is then compared to the ground truth image to compute the confusion matrix (Table 1). The arrays of this matrix are (1) True Negative (TN), the number of oil spills which were correctly predicted as oil spills, (2) False Positive (FP), the number of non-oil spills which were incorrectly predicted as oil spills, (3) False Negative, the number of oil spills which were incorrectly predicted as non-oil spills, and finally (4) True Positive (TP), the number of oil spills which were correctly predicted as oil spills (Carvalho et al., 2022).

		Predicted	
		Non-Oil	Oil
Actual	Non-Oil	True Negative (TN)	False Positive (FP)
	Oil	False Negative (FN)	True Positive (TP)

Table 1. The confusion matrix.

Then the accuracy assessment indices are derived from the confusion matrix. This study used numerical and visual analysis to assess the performance of the DenseNet model that was suggested, and then its performance was compared with a simple CNN structured algorithm. The most popular accuracy assessment indices (Seydi et al., 2022) are utilised for numerical analysis to evaluate the proposed model's effectiveness in this study (Table 2).

Criteria	Formula
N	Total number of pixels in the image
OA	$\frac{(\mathrm{TN}+\mathrm{TP})}{(\mathrm{N})}$
F1-Score	$\frac{2\mathrm{TP}}{(2TP+FP+FN}$
FAR	$\frac{(\mathrm{FP})}{(\mathrm{TN}+\mathrm{FP})}$
KC	$\frac{\frac{\mathrm{TP}}{(\mathrm{TP}+\mathrm{FP})}-\frac{(TP+FP)\times(TP+FN)+(FN+TN)\times(FP+TN)}{N^2}}{1-\frac{(TP+FP)\times(TP+FN)+(FN+TN)\times(FP+TN)}{N^2}}$
MCC	$\frac{(TP\times TN)-(FP\times FN)}{\sqrt{(TP+FP)\times(TP+FN)\times(TN+FP)\times(TN+FN)}}$

Table 2. The accuracy assessment indices.

3. CASE STUDY AND DATASET

In this study, the SAR image conducted to train and test the model is illustrated in (Figure 5). The image belongs to the oil spill that happened in the west of Cheleken Peninsula (Turkmenistan), located on the east side of the Caspian Sea. This image was captured by Sentinel-1A satellite. This scene is mainly the combination of the oil spill and non-oil (like ship and water).

The data is captured by the Sentinel-1A C-SAR sensor. The Synthetic Aperture Radar C-band is a high-resolution, all-weather sensor that captures multi-purpose images for ocean, land, and ice. The spatial resolution for this sensor is between 4 to 80 meters with a swath range of 80 to 400 km, which both depends on the operation mode. Other description of the data is written in Table 3.

Data	Date of acquisition	Resolution (m×m)	Polarization Channels
Caspian Sea	08/06/2019	10×10	VV, VH

Table 3. The description of the SAR image.

The data must be separated into evaluation, training, and testing datasets for each algorithm step. In this study, 1% and 4% of the ground truth data were used for validation and train, respectively. The model was then tested by assessing 95% of the input image.

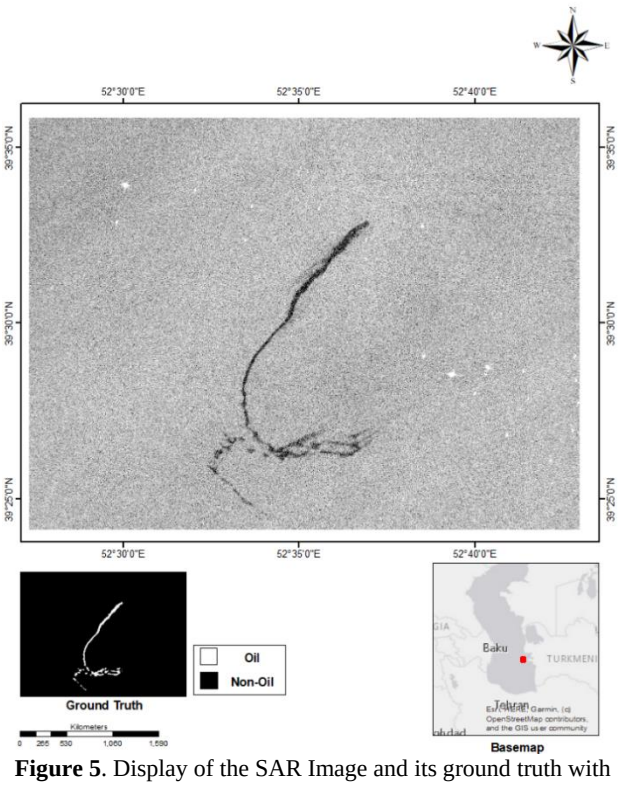

Figure 5. Display of the SAR Image and its ground truth with the approximate location of the oil spill.

4. EXPERIMENT AND RESULT

In this section, we demonstrate the outcomes of approaches, both visually and quantitatively, for better comprehension and comparison analysis. As previously stated, the results of our proposed DenseNet model is compared against a CNN algorithm, which is a common approach in image processing, particularly in

oil spill detection, and has demonstrated excellent performance in detecting oil spills in SAR images (Zhang et al., 2020).

Before the model is trained, the algorithm's hyperparameters must be specified. The following is a list of the values that were utilized for these parameters: patch-size 11×11, Adam optimizer (Kingma and Ba, 2014), binary cross entropy loss function, He-normal initializer (He et al., 2015).

4.1 Visual Comparison

One of the efficient techniques of comparison in this field is comparing the outputs of each methodology with the ground truth image of the oil spill to visually identify which parts have been miss detected or well predicted. As a result, the visual outputs are provided below (Figure 6), which white areas are the oils and black ones are representing the non-oil areas.

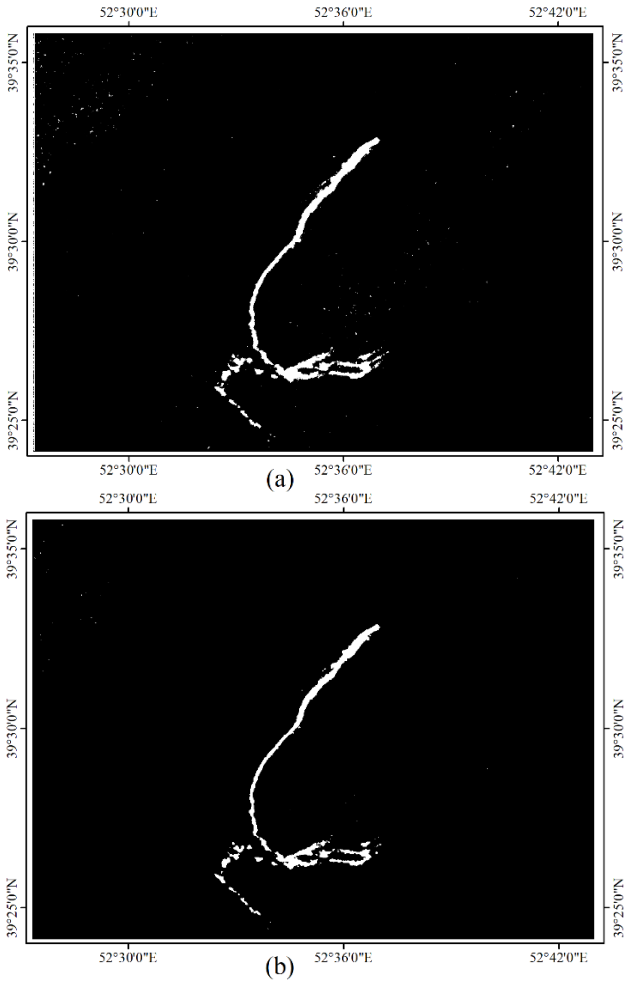

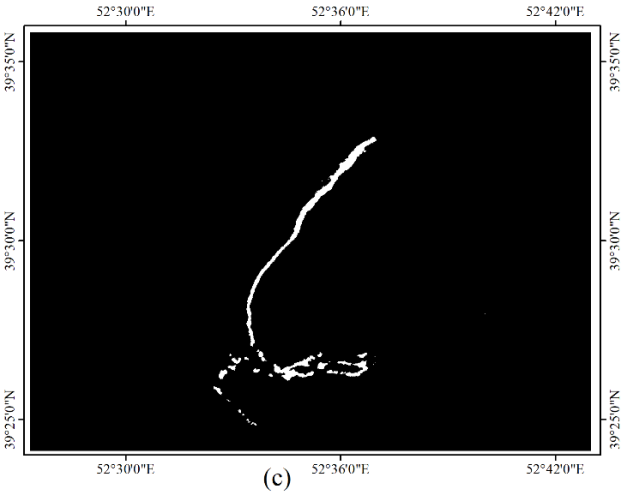

Figure 6. The outputs of CNN-based methods. The (a) common CNN method, (b) proposed DenseNet method and (c) ground truth image. The white pixels show the oil, and the black ones illustrate the non-oil.

By referencing the output images, we can state that both techniques recognized oil spills well, indicating the proper performance of deep learning in the field of oil spill detection (Seydi et al., 2021).

The results, however, have some discrepancies. The number of non-oil spills recognized as oil spills in the CNN technique output is more than that of our proposed method as it is shown that white points are indicated in places that are non-oil in the ground truth image, especially at the top left part of the image and around the actual oil spill area. As a result, it should produce more false alarms than the suggested method.

The amount of wrongly indicated oil spills are relatively low and requires more focus to be seen with the unaided eye, despite the false detection of oil spills in our suggested approach near the upper left area.

It is evident that the output of our suggested approach is far more similar to the ground truth image than the outcome of CNN's method, even with the incorrectly appointed oil spills. We may thus draw the conclusion that our suggested DenseNet technique performs better at locating oil spills.

4.2 Quantitative Comparison

The second evaluation step is to calculate and compare the accuracy indices for each approach. As was already discussed in Section 2, the arrays of the confusion matrix are used to construct the accuracy indices, which are then used to assess how well the algorithms performed. The algorithm's performance is shown by the overall accuracy (OA), which is calculated by adding the TP and TN together and dividing by the total number of observations. The result that is closest to 100% has the best performance.

A measure called F1-score is more useful than accuracy, with the optimum value of 100%. The likelihood of incorrectly predicting the real actual pixels is depicted by the false alarm rate, also known as the false positive rate alarm. If this rate is near 0, the model created a prediction that is extremely close to the ground truth image. Additionally, the Kappa coefficient, which has a maximum value of 1, is an excellent way to compare the outcomes of each approach; since it demonstrates how closely the

model classified the input picture to the ground truth image. The Matthews correlation coefficient reveals that the prediction and the ground truth image coincide perfectly with a value of 1, while the 0 and -1 values show randomly prediction and total disagreement respectively.

Criteria	CNN	DenseNet
OA (%)	99.29	99.83
F1-Score (%)	99.64	99.92
FAR	0.4313	0.0514
KCC	0.7191	0.9055
Matthews Correlation Coefficient (MCC)	0.7499	0.9065

Table 4. The accuracy assessment measurements for a standard CNN algorithm and proposed DenseNet method.

The accuracy score for each approach indicates that both detected the oil spill well; however, the variations in their function can be determined from other indices. Regarding (Table 4), the suggested DenseNet approach outperforms all of the given indices.

The considerable difference in the false alarm rate (FAR) of each strategy confirms our observation in the visualization comparison that the CNN approach has more false detection than our proposed one. DenseNet's Kappa coefficient (KCC) is at 0.9055, indicating high agreement with ground truth data (Islami et al., 2022), whereas CNN's KCC is around 0.7191. Furthermore, the Matthew correlation coefficient (MCC), a more reliable statistical rate (Chicco and Jurman, 2020), for the DenseNet approach, is greater than the CNN and near to one, indicating that the DenseNet prediction has good outcomes in all four confusion matrix categories true positive (TP), false negative (FN), true negatives (TN), and false positive (FP). Despite CNN's good performance, our proposed DenseNet technique outperformed it in identifying oil spills.

5. CONCLUSION AND DISCUSSION

A key element in maintaining the marine ecosystem, from the local inhabitants to the underwater wildlife, is the oil spill detection in the shortest amount of time with the highest level of accuracy. Therefore, tackling these issues can be greatly aided by the use of remote sensing images. Additionally, SAR data is the most useful type of remote sensing data for finding oil in ocean areas. As a result, we used a SAR image in this study to assess our approach and contrast it with a conventional convolutional neural network technique.

Additionally, the low number of polarimetric channels in a SAR image makes it challenging to detect oil spills using conventional supervised learning techniques (. i.e., Support Vector Machine). In contrast, deep learning-based approaches can extract deep features from SAR data, considerably improving the results. Although these techniques show promise in detecting oil spills, constructing an effective architecture alters each algorithm's performance, making it difficult to create an architecture that produces exceptional results. As a result, in this work we created an efficient method based on DenseNet structure. Convolution layers in this arrangement are completely interconnected by a dense block.

By detecting an oil spill using an actual SAR image of an oil spill in the Caspian Sea acquired by a Sentinel-1 sensor, the effectiveness of the suggested method was assessed. Only 5% of the ground truth data were used to train the algorithm.

As previously noted, a CNN method was used in this study to compare our findings to theirs. The results showed that both approaches offered overall accuracy of more than 99%, showing the significant potential of deep learning approaches in identifying oil spills. In terms of specifics, the proposed approach DenseNet demonstrated superior results over the CNN method in identifying oil spills and non-oil spills.

REFERENCES

Ansari, M., Homayouni, S., Safari, A., Niazmardi, S., 2021. A New Convolutional Kernel Classifier for Hyperspectral Image Classification. IEEE Journal of Selected Topics in Applied Earth Observations and Remote Sensing 14, 11240-11256.

Cantorna, D., Dafonte, C., Iglesias, A., Arcay, B., 2019. Oil spill segmentation in SAR images using convolutional neural networks. A comparative analysis with clustering and logistic regression algorithms. Applied Soft Computing 84, 105716.

Carvalho, G.d.A., Minnett, P.J., Ebecken, N.F., Landau, L., 2022. Machine-Learning Classification of SAR Remotely-Sensed Sea-Surface Petroleum Signatures—Part 1: Training and Testing Cross Validation. Remote Sensing 14, 3027.

Chicco, D., Jurman, G., 2020. The advantages of the Matthews correlation coefficient (MCC) over F1 score and accuracy in binary classification evaluation. BMC genomics 21, 1-13.

Conceição, M.R.A., de Mendonça, L.F.F., Lentini, C.A.D., da Cunha Lima, A.T., Lopes, J.M., de Vasconcelos, R.N., Gouveia, M.B., Porsani, M.J., 2021. SAR oil Spill detection system through random forest classifiers. Remote Sensing 13, 2044.

Hassani, B., Sahebi, M.R., Asiyabi, R.M., 2020. Oil spill four-Class classification using UAVSAR polarimetric data. Ocean Science Journal 55, 433-443.

He, K., Zhang, X., Ren, S., Sun, J., 2015. Delving deep into rectifiers: Surpassing human-level performance on imagenet classification, Proceedings of the IEEE international conference on computer vision, pp. 1026-1034.

Huang, G., Liu, Z., Van Der Maaten, L., Weinberger, K.Q., 2017. Densely connected convolutional networks, Proceedings of the IEEE conference on computer vision and pattern recognition, pp. 4700-4708.

Iandola, F., Moskewicz, M., Karayev, S., Girshick, R., Darrell, T., Keutzer, K., 2014. Densenet: Implementing efficient convnet descriptor pyramids. arXiv preprint arXiv:1404.1869.

Islami, F., Tarigan, S., Wahjunie, E., Dasanto, B., 2022. Accuracy Assessment of Land Use Change Analysis Using Google Earth in Sadar Watershed Mojokerto Regency, IOP Conference Series: Earth and Environmental Science. IOP Publishing, p. 012091.

Jordan, M.I., Mitchell, T.M., 2015. Machine learning: Trends, perspectives, and prospects. Science 349, 255-260.

Kingma, D.P., Ba, J., 2014. Adam: A method for stochastic optimization. arXiv preprint arXiv:1412.6980.

Orfanidis, G., Ioannidis, K., Avgerinakis, K., Vrochidis, S., Kompatsiaris, I., 2018. A deep neural network for oil spill semantic segmentation in Sar images, 2018 25th IEEE International Conference on Image Processing (ICIP). IEEE, pp. 3773-3777.

Seydi, S.T., Hasanlou, M., 2021. A new structure for binary and multiple hyperspectral change detection based on spectral unmixing and convolutional neural network. Measurement 186, 110137.

Seydi, S.T., Hasanlou, M., Amani, M., Huang, W., 2021. Oil spill detection based on multiscale multidimensional residual CNN for optical remote sensing imagery. IEEE Journal of Selected Topics in Applied Earth Observations and Remote Sensing 14, 10941-10952.

Seydi, S.T., Hasanlou, M., Chanussot, J., 2022. Burnt-Net: Wildfire burned area mapping with single post-fire Sentinel-2 data and deep learning morphological neural network. Ecological Indicators 140, 108999.

Wang, D., Wan, J., Liu, S., Chen, Y., Yasir, M., Xu, M., Ren, P., 2022. BO-DRNet: An Improved Deep Learning Model for Oil Spill Detection by Polarimetric Features from SAR Images. Remote Sensing 14, 264.

Yekeen, S.T., Balogun, A.L., Yusof, K.B.W., 2020. A novel deep learning instance segmentation model for automated marine oil spill detection. ISPRS Journal of Photogrammetry and Remote Sensing 167, 190-200.

Yu, F., Sun, W., Li, J., Zhao, Y., Zhang, Y., Chen, G., 2017. An improved Otsu method for oil spill detection from SAR images. Oceanologia 59, 311-317.

Zeng, K., Wang, Y., 2020. A deep convolutional neural network for oil spill detection from spaceborne SAR images. Remote Sensing 12, 1015.

Zhang, J., Feng, H., Luo, Q., Li, Y., Wei, J., Li, J., 2020. Oil spill detection in quad-polarimetric SAR Images using an advanced convolutional neural network based on SuperPixel model. Remote Sensing 12, 944.